J Cancer Res Clin Oncol (2016) 142:549–560
DOI 10.1007/s00432-015-2047-6

ORIGINAL ARTICLE – CANCER RESEARCH

Carfilzomib combined with suberanilohydroxamic acid (SAHA) synergistically promotes endoplasmic reticulum stress in non-small cell lung cancer cell lines

Neale T. Hanke[1] · Linda L. Garland[1] · Amanda F. Baker[1]

Received: 14 July 2015 / Accepted: 10 September 2015 / Published online: 18 September 2015

Abstract
Purpose The endoplasmic reticulum (ER) stress response is a therapeutic target for pharmacologic intervention in cancer cells. We hypothesized that combining carfilzomib (CFZ), a proteasome inhibitor, and vorinostat (SAHA), a histone deacetylase (HDAC) inhibitor, would synergistically activate ER stress in non-small cell lung cancer (NSCLC) cell lines, resulting in enhanced anti-tumor activity.
Methods Five NSCLC cell lines were treated with CFZ, SAHA, or the combination and cell proliferation measured using the MTT assay. Calcusyn software was utilized to determine the combination index as a measure of synergy. Cell viability and cytotoxicity were measured using trypan blue exclusion, CellTiter, and CytoTox assays. Western blot was used to measure markers of apoptosis, ER stress, and oxidative stress-related proteins. Reactive oxygen species (ROS) was measured using the fluorophore CM–H_2DCFDA.
Results Synergistic activity was observed for all cell lines following 48 and 72 h of combined treatment. H520 and A549 cell lines were used to assess viability and apoptosis. In both cell lines, increased death and cleaved caspase-3 were observed following combination treatment as compared with single-agent treatments. Combination therapy was associated with upregulation of ER stress-regulated proteins including activating transcription factor 4, GRP78/BiP, and C/EBP homologous protein. Both cell lines also showed increased ROS and the oxidative stress-related protein, heat shock protein 70.
Conclusion Combining proteasome inhibition with HDAC inhibition enhances ER stress, which may contribute to the synergistic anticancer activity observed in NSCLC cell lines. Further preclinical and clinical studies of CFZ + SAHA in NSCLC are warranted.

Keywords Carfilzomib · Proteasome inhibitor · Non-small cell lung cancer · SAHA

Abbreviations

ATF	Activating transcription factor
BiP	Immunoglobulin-binding protein of B cells
BTZ	Bortezomib
CFZ	Carfilzomib
CHOP	C/EBP homologous protein
CI	Combination index
DMSO	Dimethyl sulfoxide
EGFR	Epidermal growth factor receptor
ER	Endoplasmic reticulum
HDAC	Histone deacetylase
HSP70	Heat shock protein 70
MTT	3-[4,5-dimethylthiazol-2-yl]-2,5-diphenyltetrazolium bromide
NAC	N-acetyl cysteine
NSLC	Non-small cell lung cancer
PARP	Poly (ADP-ribose) polymerase
PI	Proteasome inhibitor
ROS	Reactive oxygen species
SAHA	Suberanilohydroxamic acid
SCLC	Small cell lung cancer

Electronic supplementary material The online version of this article (doi:10.1007/s00432-015-2047-6) contains supplementary material, which is available to authorized users.

✉ Amanda F. Baker
abaker@uacc.arizona.edu

[1] Section of Hematology/Oncology, College of Medicine, University of Arizona Cancer Center, 1515 N Campbell Ave, Tucson, AZ, USA

Introduction

Non-small cell lung cancer (NSCLC) is a leading cause of cancer deaths in the USA, and there is a pressing need for better therapeutic options for patients impacted by this disease. Preclinical studies suggest the proteasome is a valid therapeutic target in lung cancer (Ling et al. 2002; Teicher et al. 1999). Unfortunately, the first-generation proteasome inhibitor (PI) bortezomib (BTZ) has demonstrated relatively poor clinical activity in solid tumors, including NSCLC (Huang et al. 2014). The second-generation PI carfilzomib (CFZ) has clinical activity in BTZ refractory multiple myeloma, attributed to multiple distinct pharmacological properties including irreversible binding. Our group previously reported preclinical studies of CFZ in a diverse set of lung cancer models, showing that CFZ has potent anti-tumor activity in vitro and in vivo (Baker et al. 2014). Furthermore, initial clinical studies of CFZ have demonstrated promising anti-tumor activity in NSCLC and small cell lung cancer (SCLC), which has led to current combination studies of CFZ in SCLC (NCT01941316, NCT01987232).

Preclinical studies have demonstrated enhanced anti-tumor activity when PIs are combined with histone deacetylase (HDAC) inhibitors in a wide variety of cancer types including hematologic malignancies and solid tumors (summarized in Online Resource 1). When proteasome activity is inhibited, one outcome is that misfolded proteins can no longer be degraded through the ubiquitin–proteasome system, resulting in the formation of aggresomes that facilitate the degradation of misfolded proteins through a HDAC6-dependent mechanism (Pandey et al. 2007). Inhibition of HDAC6 results in the inability to form aggresomes making cells hypersensitive to endoplasmic reticulum (ER) stress (Kawaguchi et al. 2003; Nawrocki et al. 2006). However, recent studies suggest that HDAC6-independent ER stress-induced mechanisms may also contribute to PI plus HDAC inhibitor anti-tumor effects (Hui and Chiang 2014). Targeting ER stress in lung cancer is an attractive strategy because it is downstream of multiple growth factor signaling pathways and thus may be have broad anti-tumor activity.

Vorinostat (suberanilohydroxamic acid; SAHA) is a pan-HDAC inhibitor first approved by the US Food and Drug Administration for the treatment of cutaneous T cell lymphoma. It has activity in a number of tumor types including NSCLC. In a single-agent study of SAHA in patients with relapsed NSCLC, a benefit in time to progression was observed, but not objective responses (Traynor et al. 2009).

Based on the broad preclinical activity of second-generation CFZ in NSCLC and on favorable preclinical activity shown with combination PI and HDAC inhibition, we hypothesized that combining CFZ with SAHA might have synergistic anti-tumor activity in NSCLC cell lines. Additionally, we sought to elucidate the mechanisms by which this combination might induce ER stress and cell death.

Materials and methods

Reagents and antibodies

CFZ, provided by Onyx Pharmaceuticals, Inc., an Amgen subsidiary (South San Francisco, CA), was dissolved in dimethyl sulfoxide (DMSO) (Sigma-Aldrich) at a stock concentration of 10 mM and stored at −20 °C. SAHA was obtained from ChemieTek (Indianapolis, IN), dissolved in DMSO, and stored at −20 °C in 50 mM aliquots. A 10 mM stock of BTZ, obtained from Cell Signaling Technology (La Jolla, CA), was prepared in DMSO and stored at −20 °C. Antibodies against cleaved poly (ADP-ribose) polymerase (PARP), cleaved caspase-3, activating transcription factor 4 (ATF4), immunoglobulin-binding protein of B cells (BiP), C/EBP homologous protein (CHOP), ubiquitin and heat shock protein 70 (HSP70) were purchased from Cell Signaling Technology. Alpha-tubulin antibodies were purchased from Calbiochem (La Jolla, CA). The secondary antibodies, horseradish peroxidase (HRP)-conjugated goat anti-rabbit and HRP-conjugated goat anti-mouse, were purchased from Jackson ImmunoResearch (West Grove, PA). 5-(and 6-)chloromethyl-2′,7′-dichlorodihydrofluorescein diacetate, acetyl ester (CM–H_2DCFDA), was from Invitrogen (Carlsbad, CA). N-acetylcysteine (NAC) and cycloheximide were obtained from Sigma-Aldrich (St Louis, MO).

Cell lines

All NSCLC (NCI-H520, A549, NCI-H1993, NCI-H460, and NCI-H1299) cell lines were obtained from the American Tissue and Cell Collection (ATCC). These cells represent different pathological subtypes: squamous (H520), adenocarcinoma (H1993), and carcinoma (A549, H460, H1299). A variety of characteristics are also represented including functional p53 (A549, H460), reduced or deleted p53 (H520, H1299), functional KRAS (H1299), mutated KRAS (A549, H460), functional EGFR (A549, H460), mutated EGFR (H1993), and amplified c-met (H1993). All cells were cultured in RPMI 1640 (Cellgro) with 10 % fetal bovine serum (FBS), 1 mM sodium pyruvate, and 1X MEM nonessential amino acids. Cells were grown in 5 % CO_2 at 37 °C in a humidified tissue culture incubator. Cells were routinely tested for mycoplasma contamination using a MycoAlert mycoplasma detection kit (Lonza, Rockland, ME) and were found to be negative. To verify cell line authenticity, genomic DNA was extracted (Sigma GIN70-KT), diluted appropriately in TE buffer, and submitted to

the University of Arizona Genomics Core (Human Origins Genotyping Lab) for analysis. Autosomal short tandem repeat typing was conducted across the 13 core STRs in CODIS and referenced against allelic peaks in cell lines of previously confirmed genotype. All cell lines were verified as authentic.

Proliferation assay

Cells (5×10^3) were seeded in 96-well plates and incubated overnight. Concentrated drug was added to existing media, exposing the cultures to various concentrations of CFZ and/or SAHA for the specified treatment intervals. Control cells for CFZ were mock treated with 0.01 % DMSO, and control cells for SAHA were mock treated with 0.1 % DMSO. The resulting proliferation of cells was determined by 3-[4,5-dimethylthiazol-2-yl]-2,5-diphenyltetrazolium bromide (MTT) assay. MTT dye (1 mg/ml) was added, and the cells were incubated for an additional 4 h at 37 °C. After removal of medium, the formazan crystals were dissolved in DMSO for 5 min by shaking and the plates were read in a spectrophotometer at 540 nm. Dose–response curves were created using GraphPad Prism version 5.01 (GraphPad Software Inc, La Jolla, CA). The half maximal inhibitory concentration (IC_{50}) values were calculated using CalcuSyn (Biosoft, Great Shelford, Cambridge, UK).

Drug combination studies

Cells were seeded as described in the proliferation assay section and treated with various concentrations of CFZ and SAHA simultaneously for 48 or 72 h before being analyzed. The concentration range used for CFZ was 0.15 nM to 1 μM, and the concentration range used for SAHA was 7.6 nM to 50 μM. Interactions between CFZ and SAHA were analyzed using the median effect method of Chou and Talalay (1983). With this method, dose–response curves are generated for each agent individually. These results are then used to analyze the results obtained from the combination treatment. A combination index (CI) was generated using CalcuSyn software (Biosoft, Cambridge, United Kingdom), and synergy-level classifications were assigned as described in the CalcuSyn manual. A CI of <1 indicates synergy (<0.3, strong synergy), a CI of 1 indicates additive effects, and a CI of more than 1 is indicative of antagonistic effects (>3, strong antagonism).

Western blot analysis

After treatment, the cells were rinsed with cold phosphate-buffered saline (PBS) and harvested in a buffer containing 50 mM Tris–HCl (pH 8.0), 150 mM NaCl, 1 % Triton X-100, 2 mM EDTA, 5 mM Na_3VO_4, 200 μM NaF, 21 μM leupeptin, 230 nM aprotinin, and 1 mM phenylmethylsulfonyl fluoride (PMSF). The cell lysate was sonicated and centrifuged at $10{,}000 \times g$ for 10 min at 4 °C. Protein concentration of the resulting supernatant was determined using a 660 nm Protein Assay kit (Thermo Scientific, Rockford, IL). Twenty micrograms of total cell lysate was boiled for 5 min and resolved in a 10 or 16 % acrylamide/bisacrylamide gel by electrophoresis at 125 V for 105 min. Proteins were then transferred to a polyvinylidene fluoride (PVDF) membrane (Millipore, Billerica, MA). Membranes were blocked with 5 % milk in Tris-buffered saline containing 0.1 % Tween-20 (TBST) for 30 min before overnight incubation at 4 °C with various primary antibodies, typically at a 1:1000 dilution. Blots were rinsed with TBST and incubated for 2 h at room temperature with secondary antibody at a 1:15,000 dilution. Reactive bands were visualized by exposure to film using Pierce Supersignal West Pico HRP Detection Reagent (Thermo Fisher Scientific, Rockford IL). Blots were stripped with One Minute Plus Western Blot Stropping Buffer (GM Biosciences) before reprobing with additional primary and secondary antibodies.

Cell viability/cytotoxicity assays

To measure the percent of viable vs dead cells, trypan blue staining was performed. Cells (6×10^5) were seeded in 6-well plates and incubated overnight. Cultures were left untreated or treated with predetermined 48 h IC_{50} doses of CFZ, BTZ, SAHA or combinations and incubated for an additional 48 h. The media containing any non-adherent cells was then collected. Adherent cells were detached using trypsin, suspended in culture medium, and disaggregated by manual pipetting. After mixing all collected cells with trypan blue (Thermo Scientific), viable cells that excluded the dye and dead cells that stained an intense blue were counted using a hemocytometer. To analyze cell viability based on ATP, cells (5×10^3) were seeded in 96-well white-walled plates and incubated overnight. Cells were left untreated or treated with predetermined 48-h IC_{50} doses of CFZ, BTZ, SAHA, or combinations. After 48 h, the CellTiter-Glo kit (Promega) was used according to the manufacturer's instructions. Luminescence was measured by a Beckman Coulter Multimode DTX880 microplate reader. Values are presented as percent of control. Cell cytotoxicity based on detection of intracellular protease activity (dead-cell protease) was performed using the CytoTox-Glo assay (Promega). Cells (5×10^3) were seeded in 96-well white-walled plates and incubated overnight. Predetermined 48-h IC_{50} doses of CFZ, BTZ, SAHA, or combinations were applied to the cells. Following a further 48-h incubation, the CellTox-Glo kit was used according to the manufacturer's instructions. Luminescence was measured

by a Beckman Coulter Multimode DTX880 microplate reader. Values are presented as a percent of control.

Flow cytometry

Cell death was analyzed with the annexin V–fluorescein isothiocyanate (FITC) apoptosis detection kit (Sigma-Aldrich, St. Louis, MO) according to the manufacturer's instructions. Cells were seeded in 100-mm plates and incubated overnight. Treatment media was added, and the plates were incubated an additional 48 h. Both floating and adherent cells were collected and washed in PBS. The cells were analyzed by flow cytometry following incubation with annexin V–FITC and propidium iodide (FACSCanto II, BD Biosciences, San Jose, CA). Data analysis was performed using FlowJo software (Treestar Inc., Ashland, OR).

Reactive oxygen species (ROS) measurement

The measurement of ROS was taken using the cell-permeable probe CM–H_2DCFDA (C6827) from Molecular Probes, Invitrogen. Cells (6×10^5) were seeded overnight in 6-well plates. The ROS indicator was then applied at 1 μM for 30 min at 37° C. The CM–H_2DCFDA dye was removed, and the cells washed twice with PBS. Cells were then cultured with media alone or media containing predetermined IC_{50} doses of CFZ, BTZ, SAHA, or combinations. After 48 h, the cells were collected, rinsed with PBS, and lysed. Fluorescence was determined using a Beckman Coulter Multimode DTX 880 microplate reader with excitation at 485 nm and emission at 520 nm. Protein concentration was determined using the 660 nm Protein Assay kit, and values were normalized to protein content.

Statistical analysis

The error bars shown for all data depict the standard deviation from the mean. Statistical significance between groups was performed using a two-tailed, unpaired Student's *t* test in Microsoft Excel (Microsoft Corporation, Redmond, WA).

Results

CFZ and SAHA act synergistically to suppresses proliferation in a range of NSCLC cell lines

Using a panel of 5 cell lines, we modeled the anti-tumor effects of CFZ + SAHA treatment in non-small cell lung cancer. The cell line sensitivity to CFZ, SAHA, and the combination was profiled by the MTT assay at 48 and 72 h of treatment. Results from one representative experiment ($n = 6$) following 72 h of treatment are shown in Fig. 1. For each of the cell lines tested, the combination treatment of CFZ + SAHA was more potent in inhibiting cell growth than either compound alone. Growth curves at 48 h were similar to the 72-h curves (data not shown). IC_{50} values were calculated from the 48- and 72-h growth curves and are displayed in Table 1. The IC_{50} values for cell lines treated with CFZ were in the low nanomolar range in contrast to IC_{50} values in the micromolar range for the cell lines treated with SAHA. Average CI values, calculated from the growth inhibition rates of 50, 75, 90, and 95 %, confirm synergism in all cell lines at both 48 and 72 h. To further investigate the molecular and cellular effects of the CFZ and SAHA combination, we selected two cell line models, the H520 and A549 cells, for additional analysis.

Combination treatment of CFZ + SAHA enhances the accumulation of ubiquitinated proteins

Since polyubiquitinated proteins are efficiently degraded by cellular proteasomes, the accumulation of ubiquitin conjugates can be used as a reflection of proteasome inhibition. To examine the accumulation of ubiquitin conjugates, Western blot analysis was performed on H520 and A549 cells treated for 24 h with CFZ, SAHA, or the combination. For these studies, the predetermined 48-h IC_{50} values were used as drug treatment doses and BTZ was included for comparison purposes. Figure 2 shows an absence of ubiquitin conjugates in untreated and SAHA-treated cells, indicative of normal proteasome activity. Cells treated with the proteasome inhibitor CFZ, as expected, show an accumulation of ubiquitin conjugates. Interestingly, cells treated with the CFZ + SAHA combination show an additional accumulation of ubiquitin conjugates above that of cells treated with CFZ alone. Similar results were observed with BTZ.

CFZ + SAHA combination treatment reduces cell viability

To examine the effect of CFZ and SAHA on cell viability, H520 and A549 cells were exposed to predetermined 48-h IC_{50} doses. BTZ was utilized for comparison purposes. Cells were collected at 48 h and analyzed using trypan blue exclusion. Figure 3a displays the result of one experiment ($n = 3$). We did not observe a substantial decrease in viable cells with single-agent CFZ treatment compared to the control, suggesting that much of the 50 % affected fraction at the IC_{50} dose may be due to reduced cell proliferation rather than cell death. There was, however, a strong sensitivity to CFZ + SAHA

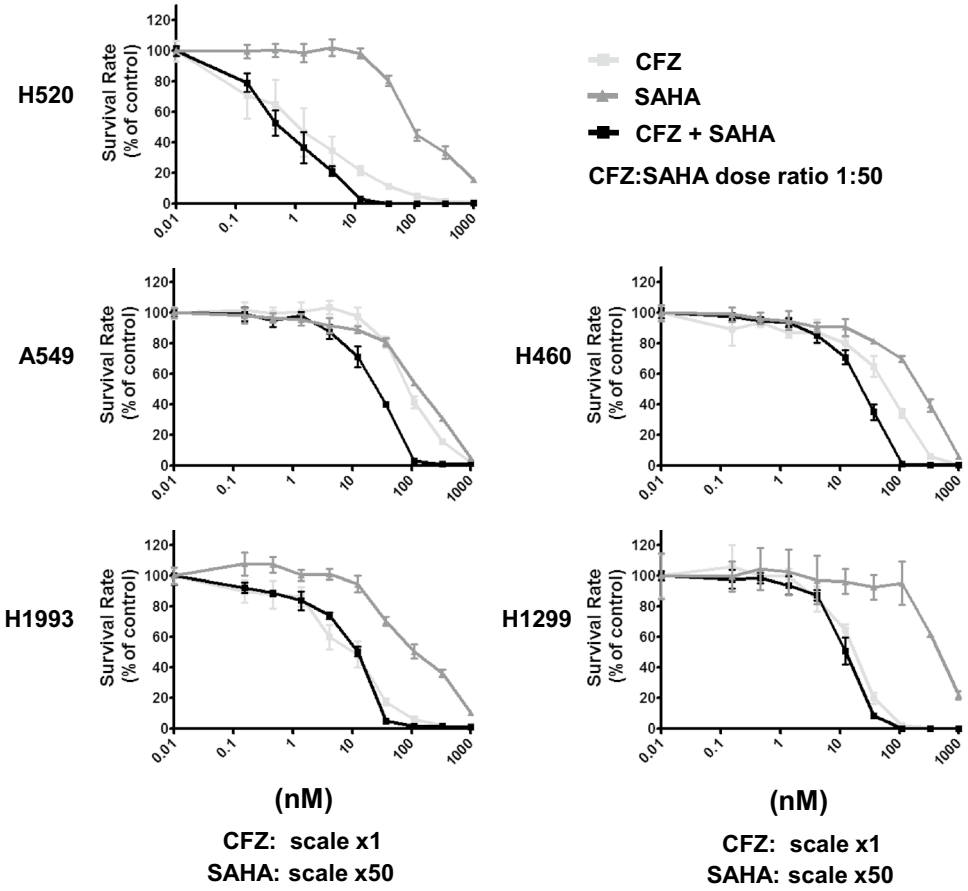

Fig. 1 Dose–response curves illustrate the effect of CFZ and SAHA, alone and in combination, on the growth of NSCLC cell lines. Cells were exposed to CFZ, SAHA, or the combination, at various concentrations for 72 h and assayed by MTT as described in Materials and Methods section. One representative experiment is shown, $n = 6$

Table 1 Sensitivity of NSCLC cell lines to CFZ and SAHA

Cell line	CFZ IC_{50} (nM)		SAHA IC_{50} (nM)		CFZ + SAHA IC_{50} (nM)		Combination index	
	48 h	72 h	48 h	72 h	48 h	72 h	48 h	72 h
H520	15.13	1.10	20,251	8941	8.13	0.59	0.30	0.26
A549	127.30	104.80	6871	6340	11.38	17.89	0.19	0.29
H1993	12.94	5.36	8103	6827	6.66	4.40	0.35	0.68
H460	56.50	41.21	10,448	7203	22.06	20.82	0.21	0.33
H1299	8.03	16.30	25,609	24,418	10.52	11.46	0.87	0.76

The determined inhibitory concentrations (IC_{50} values) represent the level of drug that inhibited cell growth by 50 %. IC_{50} values (nM) are the mean of one experiment, $n = 6$. Combination index (CI) values were obtained by the method described by Chou and Talalay (1983). Values shown are an average CI from a single experiment at growth inhibition rates of 50, 75, 90, and 95 %. CI interpretation: <0.3 = strong synergism, 0.3–0.7 = synergism, 0.7–0.9 = moderate to slight synergism, 0.9–1.1 = nearly additive, 1.1–1.45 slight to moderate antagonism

combination therapy with a significant decrease in viable cells as compared to single-agent-treated cells. Similar results were observed with BTZ in the H520 cells; however, the BTZ + SAHA treated A549 cells did not have significantly decreased viability compared to their respective single-agent-treated groups. To further substantiate these results, cells were again treated for 48 h and then analyzed with the Promega CellTiter-Glo viability assay. This luminescence-based assay uses quantification of ATP to determine the presence of metabolically active cells. The results are shown in Fig. 3b with values presented as a percent of control. This assay also showed a significant decrease in metabolically active cells in the CFZ + SAHA combination-treated group as compared with the single-agent-treated groups. Similar trends were observed with BTZ.

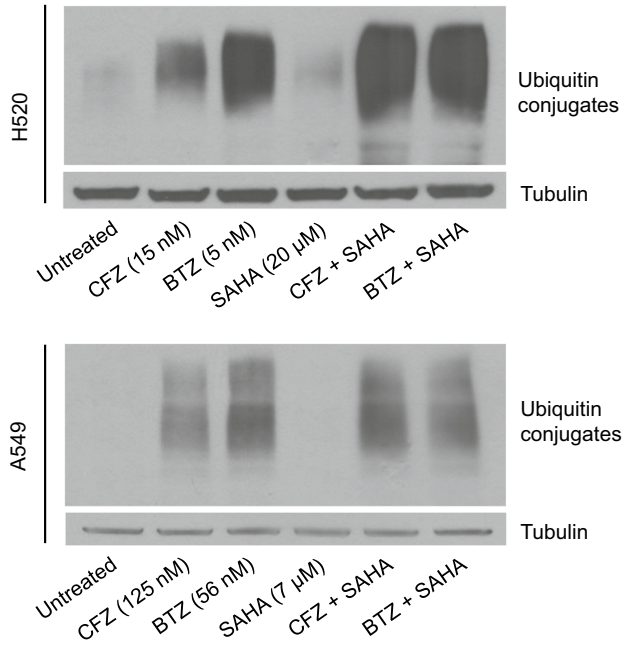

Fig. 2 Effect of CFZ and SAHA treatment on the accumulation of ubiquitinated proteins. Cells were left untreated or treated as indicated with 48-h IC_{50} doses. Detection of ubiquitinated proteins was determined by immunoblot in total extracts of cells harvested at 24 h. BTZ treatments are shown for comparison purposes, and α-tubulin is shown as a loading control

CFZ + SAHA treatment induces cytotoxicity and markers of apoptosis

Next, we investigated whether the observed reduction in cell viability that occurs with CFZ + SAHA combination treatment involved cytotoxicity and the induction of apoptosis. BTZ was again included as a control. To determine whether combination treatment causes release of "dead-cell protease activity," the Promega CellTox-Glo cytotoxicity assay was performed. Reagents were added to 48-h treated cells according to the manufacturer's instructions. The results using both H520 and A549 cells are shown in Fig. 4a. Induced cytotoxicity was significantly higher in the CFZ + SAHA combination-treated cells versus the single-agent-treated cells. Lysate from cells treated for 24 h were also collected and analyzed by Western blot to probe for markers of apoptosis. In both the H520 and A549 cells, high levels of cleaved caspase-3 and cleaved PARP were detected in the CFZ + SAHA combination-treated cells (Fig. 4b). Similar results were observed with BTZ. To further evaluate levels of apoptosis, 48-h treated cells were also stained for annexin V and propidium iodide and analyzed by flow cytometry. Figure 4c shows a substantial increase in apoptotic cells for the CFZ + SAHA combination-treated cells versus the single-agent-treated cells in both cell lines. As with trypan blue exclusion (Fig. 3a), the

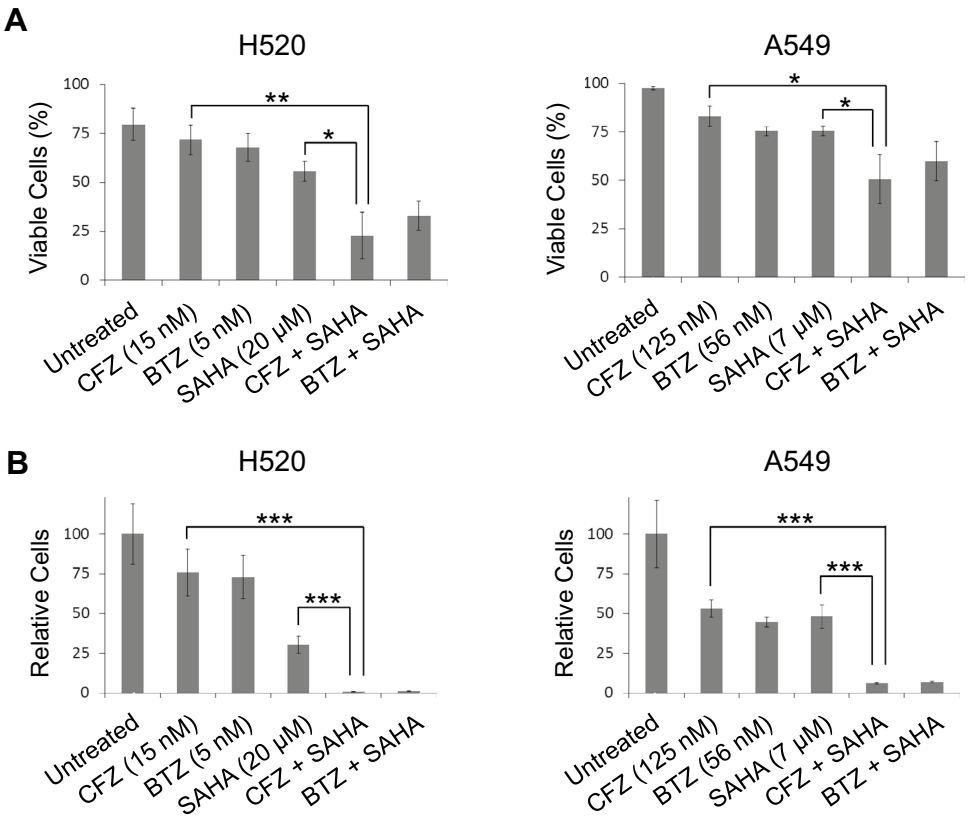

Fig. 3 CFZ and SAHA treatment reduces cell viability. Cells were left untreated or treated as indicated for 48 h with 48-h IC_{50} doses. **a** Viability was determined by direct cell counting after trypan blue staining. ±SD are shown ($n = 3$). **b** The CellTiter-Glo cell viability assay was used to determine the number of viable cells based on quantitation of ATP by metabolically active cells. The number of untreated cells was considered to be 100. ±SD are shown ($n = 6$). BTZ treatments are shown for comparison purposes. *, ($p < 0.05$); **, ($p < 0.005$); ***, ($p < 0.0005$)

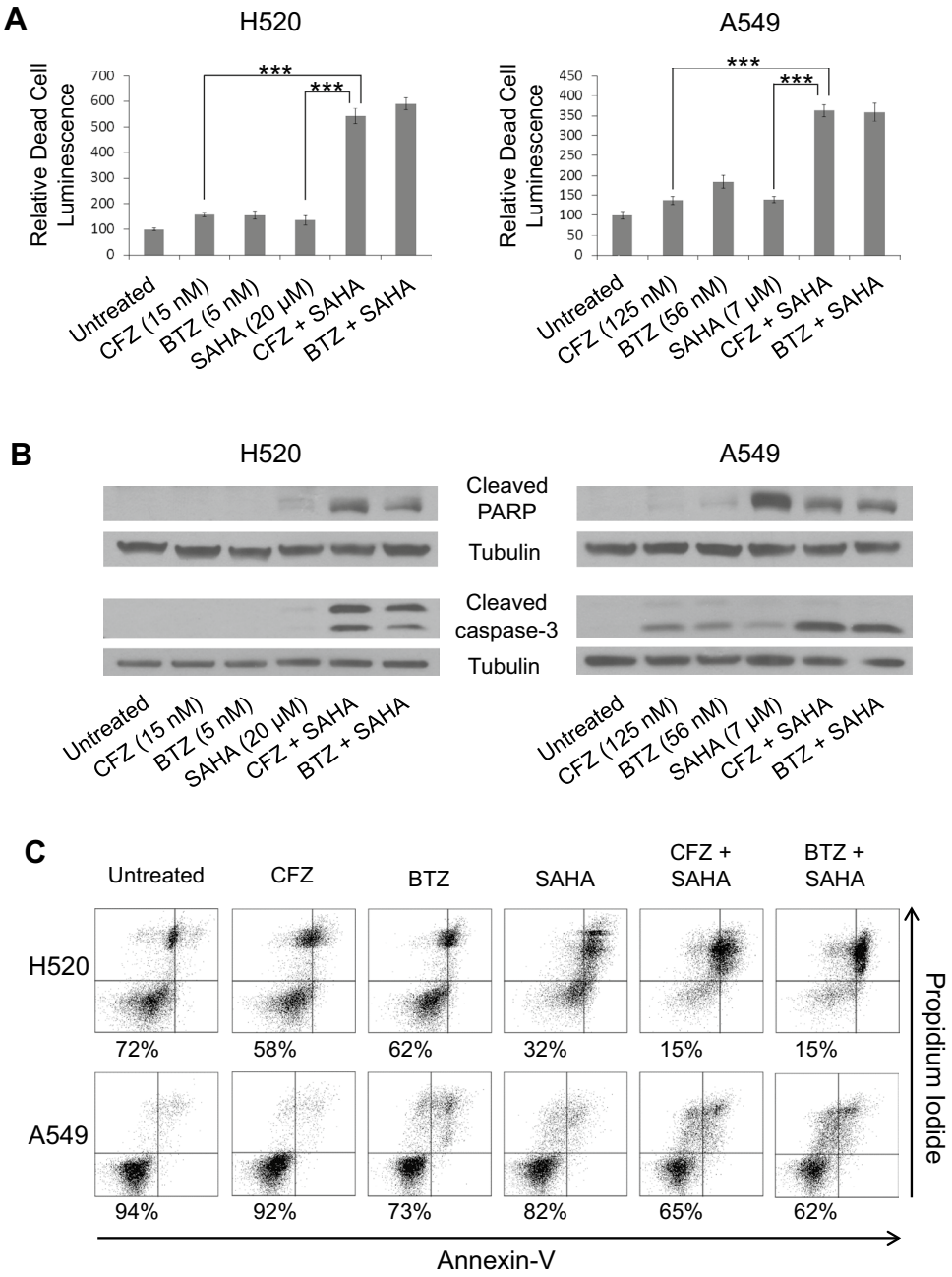

Fig. 4 Treatment with CFZ and SAHA induces cytotoxicity and markers of apoptosis. Cells were left untreated or treated as indicated with 48-h IC_{50} doses. **a** Detection of dead cells was measured with CytoTox-Glo assay. ±SD are shown ($n = 6$). Results are presented relative to untreated controls. ***, ($p < 0.0005$). **b** Detection of cleaved PARP and cleaved caspase-3 by immunoblot in total extracts of cells harvested at 24 h. α-Tubulin is shown as a loading control. **c** Determination of apoptosis after 48 h of treatment using annexin V and propidium iodide staining. The percentage of viable cells (annexin V negative, propidium iodide negative) is displayed. BTZ treatments are shown for comparison purposes

flow analysis did not reveal a substantial decrease in viable cells with single-agent CFZ treatment compared to the control, suggesting that treatment at the IC_{50} dose is reducing cell proliferation rather than inducing cell death.

Combination CFZ + SAHA treatment induces endoplasmic reticulum and oxidative stress

To determine whether ER stress is induced with the synergistic action of CFZ + SAHA, various markers of ER stress were evaluated by Western blot analysis on both the H520 and A549 cells with BTZ used as a control. Transcription of ATF4 is upregulated by the unfolded protein response (Harding et al. 2000). In turn, the ATF4 transcription factor activates transcription of CHOP in the integrated ER stress response (Fawcett et al. 1999). The chaperone protein BiP is also an indicator of ER stress conditions (Lee 2005). Each of these three ER stress markers (ATF4, CHOP, and BiP) was found to be highly upregulated in the whole cell lysate of CFZ + SAHA treated cells as compared to single-agent-treated cells (Fig. 5a). Similar results were observed with BTZ.

Next, we evaluated the induction of oxidative stress and the formation of ROS by using the CM–H_2DCFDA probe.

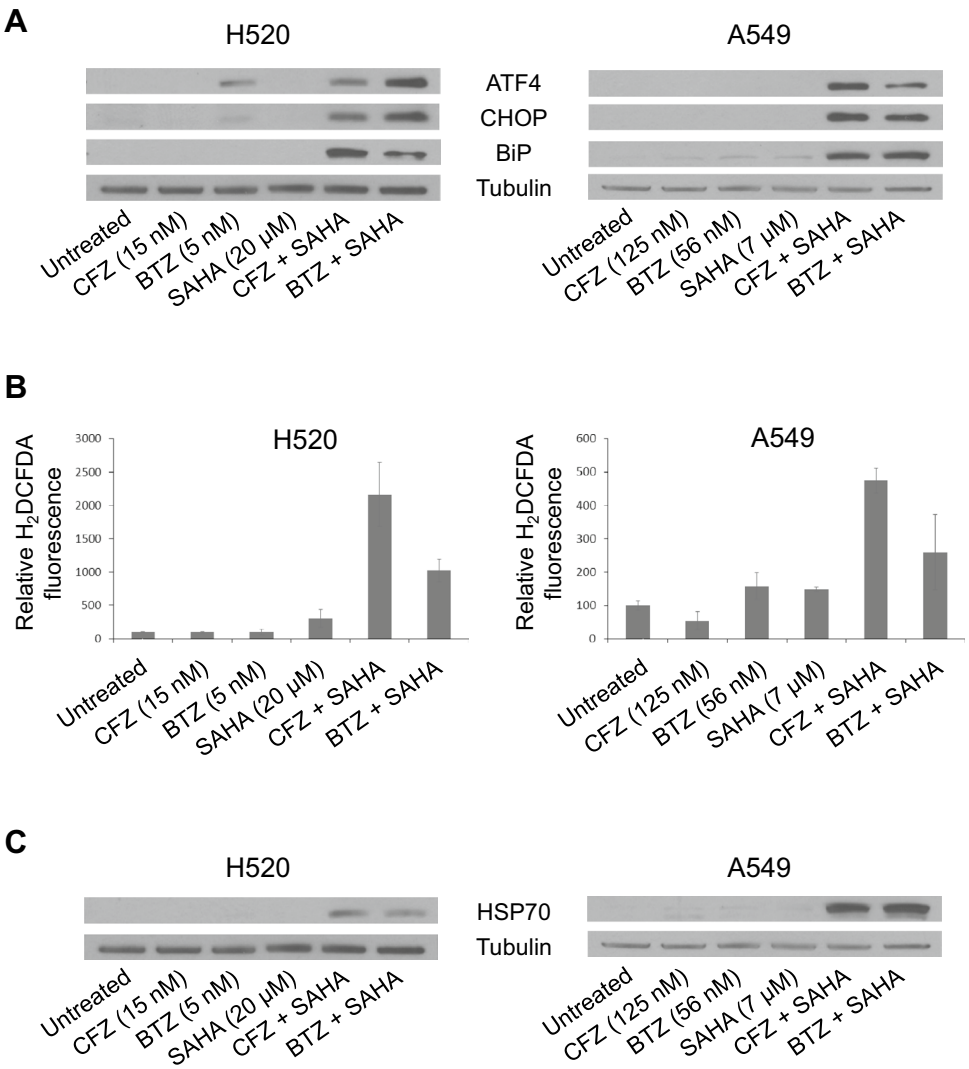

Fig. 5 CFZ and SAHA act synergistically to induce endoplasmic reticulum and oxidative stress. Cells were left untreated or treated as indicated with 48-h IC_{50} doses. **a** Detection of an ER stress-related proteins (ATF4, CHOP, and BiP) by immunoblot in total extracts of cells harvested at 24 h. α-Tubulin is shown as a loading control. **b** Relative ROS was measured from cells harvested at 24 h using the CM-H_2DCFDA fluorescence probe. Values are normalized to protein content and displayed relative to the untreated control. **c** Detection of oxidative stress protein (HSP70) by immunoblot in total extracts of cells harvested at 24 h. α-Tubulin is shown as a loading control. BTZ treatments are shown for comparison purposes

This membrane-permeable probe becomes fluorescent upon oxidation. Analysis of H520 and A549 cells showed increased fluorescence in the CFZ + SAHA treated groups as compared to the untreated or single-agent-treated groups, reflecting induced oxidative stress (Fig. 5b). HSP70 expression has been shown to be upregulated with oxidative stress (Su et al. 1998). Figure 5c shows Western blot analysis of HSP70 with strong induction seen in the CFZ + SAHA combination-treated group compared to the untreated or single-agent-treated groups. Similar trends were observed with BTZ.

ROS generated from CFZ + SAHA treatment does not significantly contribute to the ER stress response or loss of cell viability

To examine whether the increased intracellular ROS that occurs with CFZ + SAHA treatment is an important component in the ER stress response, we utilized the antioxidant, N-acetyl cysteine (NAC). Groups of H520 and A549 cells were pretreated for 5 h with doses of NAC. The NAC media was removed, and the cells were then left untreated or treated with CFZ + SAHA for an additional 24 h before harvest. Western blot analysis showed that pretreatment of NAC did not alter the amount of ubiquitin conjugates that are induced with CFZ + SAHA treatment (Fig. 6a). Increasing doses of NAC did reduce HSP70, indicative of a reduction in ROS (Fig. 6b). However, markers of ER stress (ATF4, BiP, and CHOP) and apoptosis (cleaved caspase-3) were not altered in a dose-dependent manner, although they were somewhat abrogated at the highest dose of NAC. Cell viability was also measured by trypan blue exclusion. Pretreatment with NAC did not rescue cell viability in the CFZ + SAHA group (Fig. 6c).

Induced ER stress with CFZ + SAHA treatment requires protein synthesis

Cycloheximide, a protein synthesis inhibitor, was used to validate a link between the accumulation of ubiquitinated

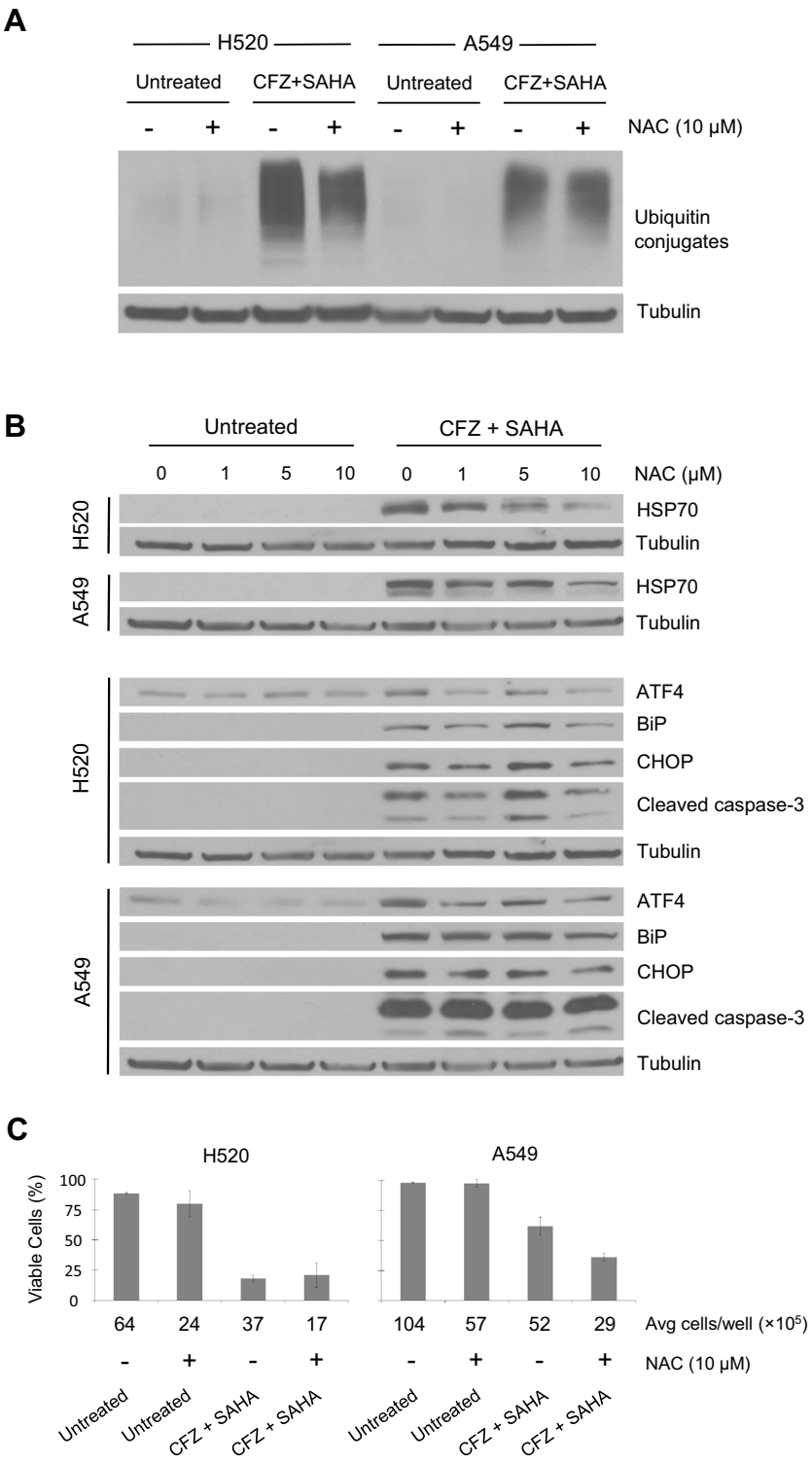

Fig. 6 ROS generated with CFZ and SAHA treatment does not significantly contribute to ER stress and cytotoxicity. Cells were pretreated for 5 h with vehicle (4 % PBS) or concentrations of NAC as indicated. Pretreatment media was removed, and cells were either left untreated or treated with CFZ + SAHA 48-h IC_{50} doses. Western blot analysis of total cell lysate harvested at 24 h was used to detect **a** ubiquitinated proteins and **b** oxidative stress, ER stress, and apoptosis-related proteins. α-Tubulin is shown as a loading control. **c** Cell viability was determined after 48 h of treatment by direct counting with trypan blue staining. ±SD are shown ($n = 3$)

proteins and ER stress. H520 and A549 cells were pretreated with 10 μg/ml cycloheximide for 4 h. The cycloheximide media was removed, and the cells were then left untreated or treated with CFZ + SAHA for an additional 24 h before harvest. Evaluation by Western blot showed that cycloheximide pretreatment blocked the accumulation of ubiquitin conjugates that are induced by CFZ + SAHA treatment (Fig. 7a). Western analysis also showed a substantial reduction in the markers of ER stress (ATF4, BiP, and CHOP) and cleaved caspase-3 when the CFZ + SAHA cells are pretreated with cycloheximide (Fig. 7b). Cell viability was examined by trypan blue exclusion following

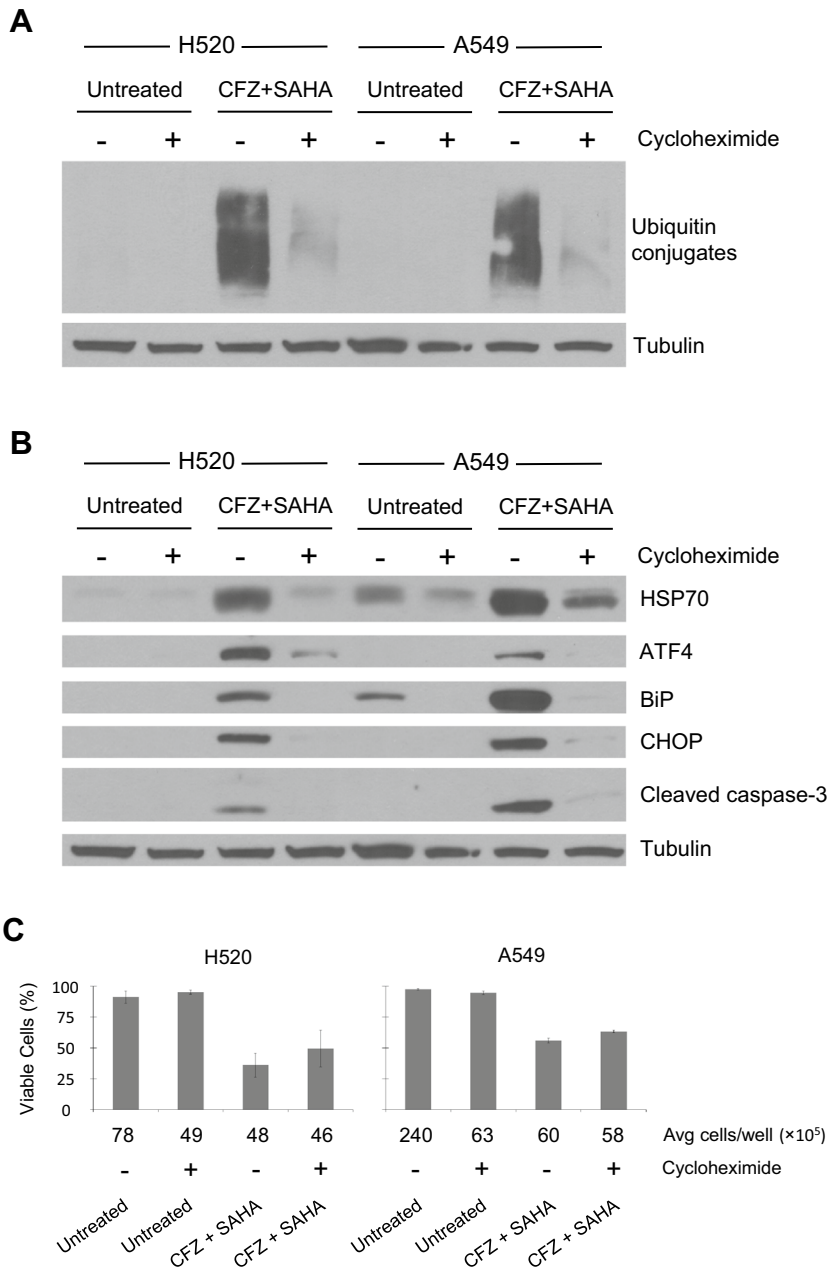

Fig. 7 Induced ER stress with CFZ and SAHA treatment requires protein synthesis. Cells were either mock (DMSO 0.1 %) or cycloheximide (10 μg/ml) treated for 4 h. Pretreatment media was removed, and cells were left untreated or treated with CFZ + SAHA 48-h IC_{50} doses. Detection of **a** ubiquitin conjugates and **b** oxidative stress, ER stress, and apoptosis-related proteins by immunoblot in total extracts of cells harvested at 24 h. α-Tubulin is shown as a loading control. **c** Cell viability at 48 h was determined by direct cell counting after trypan blue staining. ±SD are shown ($n = 3$)

48 h of treatment (Fig. 7c). The pretreatment of cycloheximide alone was found to reduce cell number from 37–75 %. Considering this reduced proliferation, comparison of the two CFZ + SAHA treated groups did not show a significant improvement in cell viability (H520 p value: 0.26, A549 p value: 0.08). However, the trend is suggestive of a possible link between interrupted protein synthesis and improved cell viability following CFZ + SAHA treatment. This is consistent with other single-agent treatment studies that find cycloheximide attenuates cytotoxicity in cells treated with BTZ (Moriya et al. 2013) or HDAC inhibitors (Bolden et al. 2006).

Discussion

We studied the combination of CFZ, a second-generation PI, with the HDAC inhibitor SAHA in a panel of NSCLC cell lines. Based on prior preclinical studies, we hypothesized that CFZ + SAHA might synergistically target ER stress. Our results indicate that the addition of SAHA markedly potentiates the anti-proliferative activity of CFZ in lung cancer cell line models. Although a range of single-agent CFZ IC_{50} values was observed across the five molecularly diverse cell lines tested, a consistent trend for synergy with SAHA was observed for all cell lines at both 48

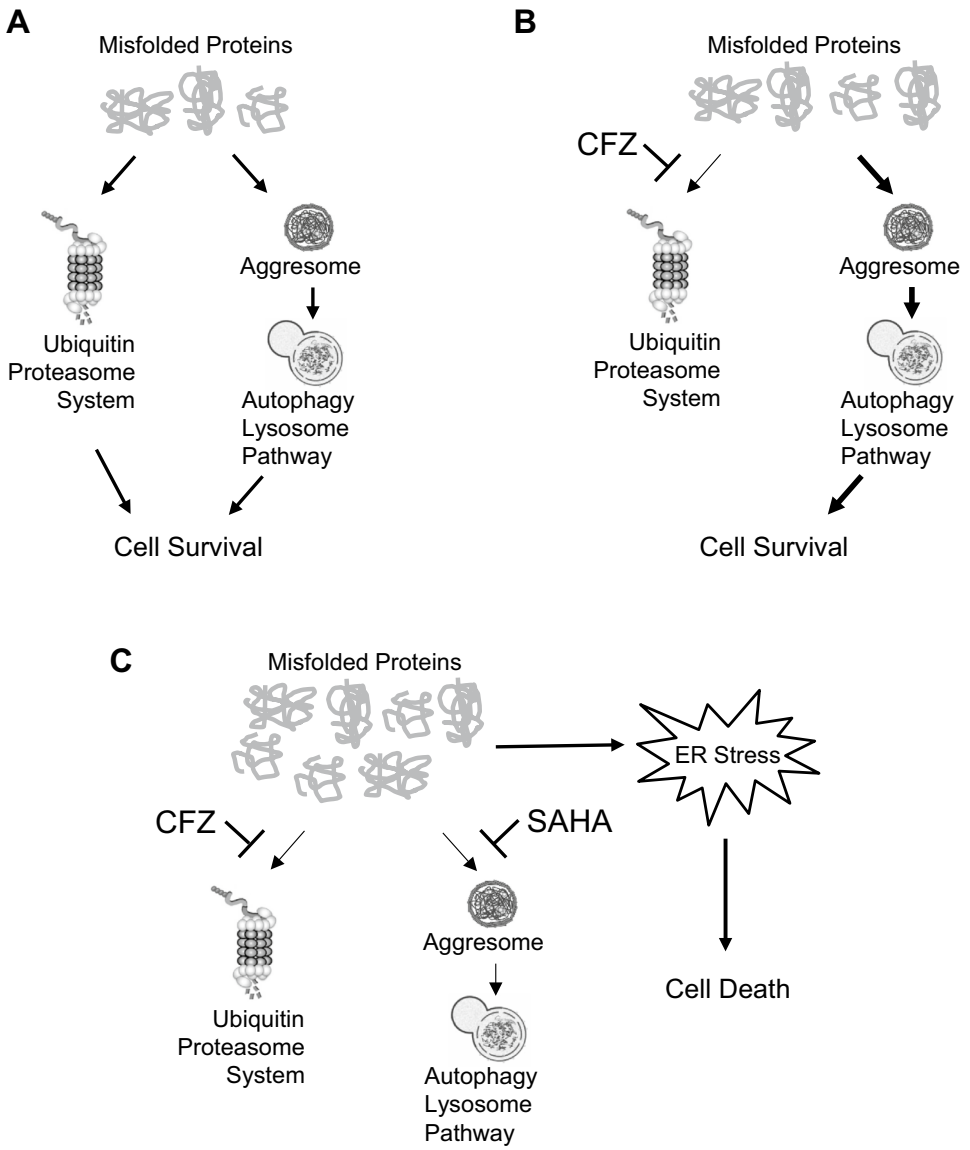

Fig. 8 Proposed illustration of protein degradation pathways in lung cancer cells. **a** Untreated cells utilize two intracellular catabolic pathways for the removal of misfolded proteins. **b** As CFZ blocks the ubiquitin proteasome system, resistant cells degrade misfolded proteins through increased use of the autophagy-lysosome pathway. **c** Blocking the two major degradation pathways with CFZ + SAHA treatment results in the accumulation of misfolded proteins, ER stress, and cell death

and 72 h of treatment. Our results in NSCLC are similar to observations of synergy that have been made in non-Hodgkin lymphoma models where the HDAC6 inhibitor ricolinostat was synergistic with CFZ (Dasmahapatra et al. 2014), in mantle cell lymphoma (MCL) where SAHA and SNDX-275 were shown to be synergistic with CFZ (Dasmahapatra et al. 2011), and in head and neck carcinoma models where HDAC inhibitors were shown to be synergistic with CFZ (Zang et al. 2014). Comparable to the observations made in MCL, we observed an increase in ROS when SAHA was combined with CFZ. Many HDAC inhibitors including SAHA induce ROS and result in elevated levels of the redox-sensitive NF-κB, which can mediate cell survival. In a recent study by Karthik et al. (2015) in NSCLC cell lines, proteasome inhibition using BTZ diminished I-κB degradation preventing NF-κB activation and translocation, suggesting that inhibition of NF-κB may be one mechanism contributing to synergy of this combination. In our study, treatment with the antioxidant NAC did not rescue cells from death induced by the combination of CFZ and SAHA, indicating that ROS generation was not a predominant mechanism by which this combination led to cell death.

Our studies showed that CFZ and SAHA when combined disrupted the process by which misfolded proteins are removed from the cell, leading to excessive ER stress and thereby, the induction of apoptosis (Fig. 8). Autophagy is a survival mechanism activated in response to UPR stress that can result in drug resistance. We did not investigate the induction of autophagy in response to the combination of CFZ and SAHA. However, in earlier studies we have shown that CFZ alone can induce expression of LC3B-II, a marker of autophagy, in lung cancer cell lines (Baker et al. 2014). Inhibition of autophagy has been shown to enhance other therapeutic combinations, including those that incorporate

proteasome inhibitors or HDAC inhibitors, and thus may represent a strategy to further enhance the efficacy of CFZ combined with SAHA.

NSCLC is characterized by genetic variability resulting in refractory or drug-resistant phenotypes. Therapeutic strategies that target tumor phenotypes, rather than highly specific genotypes, are therefore an attractive strategy in this disease. Our study showed synergistic anti-tumor activity across a broad range of NSCLC cell lines and suggests that ER stress appears to be a relevant target in NSCLC. In a study of SAHA and BTZ as a third-line therapy in patients with advanced NSCLC, no clinical activity was observed (Hoang et al. 2014). Therefore, further work is needed to identify biomarkers to enrich for patients most likely to benefit from a CFZ + SAHA.

Acknowledgments The authors wish to thank the University of Arizona Cancer Center/Arizona Research Laboratories (UACC/ARL) Cytometry Core Facility for their assistance with this study.

Compliance with ethical standards

Funding This work was supported by a generous gift from the late Mrs. Jemmie Helmricks and her husband, a research collaboration award by Onyx Pharmaceuticals, Inc., an Amgen subsidiary, and a Basic/Clinical translational partnership pilot grant award from the Arizona Cancer Center Support Grant P30CA023074 from the National Cancer Institute (NCI).

Conflict of interest All authors declare no conflict of interest.

Ethical approval This article does not contain any studies with human participants or animals performed by any of the authors.

Informed consent No human participants were used in this study.

References

Baker AF, Hanke NT, Sands BJ, Carbajal L, Anderl JL, Garland LL (2014) Carfilzomib demonstrates broad anti-tumor activity in pre-clinical non-small cell and small cell lung cancer models. J Exp Clin Cancer Res: CR 33:111

Bolden JE, Peart MJ, Johnstone RW (2006) Anticancer activities of histone deacetylase inhibitors. Nat Rev Drug Discov 5:769–784

Chou TC, Talalay P (1983) Analysis of combined drug effects: a new look at a very old problem. Trends Pharmacol Sci 4:450–454

Dasmahapatra G et al (2011) Carfilzomib interacts synergistically with histone deacetylase inhibitors in mantle cell lymphoma cells in vitro and in vivo. Mol Cancer Ther 10:1686–1697

Dasmahapatra G, Patel H, Friedberg J, Quayle SN, Jones SS, Grant S (2014) In vitro and in vivo interactions between the HDAC6 inhibitor ricolinostat (ACY1215) and the irreversible proteasome inhibitor carfilzomib in non-Hodgkin lymphoma cells. Mol Cancer Ther 13:2886–2897

Fawcett TW, Martindale JL, Guyton KZ, Hai T, Holbrook NJ (1999) Complexes containing activating transcription factor (ATF)/cAMP-responsive-element-binding protein (CREB) interact with the CCAAT/enhancer-binding protein (C/EBP)-ATF composite site to regulate Gadd153 expression during the stress response. Biochem J 339(Pt 1):135–141

Harding HP, Novoa I, Zhang Y, Zeng H, Wek R, Schapira M, Ron D (2000) Regulated translation initiation controls stress-induced gene expression in mammalian cells. Mol Cell 6:1099–1108

Hoang T et al (2014) Vorinostat and bortezomib as third-line therapy in patients with advanced non-small cell lung cancer: a Wisconsin Oncology Network Phase II study. Investig New Drugs 32:195–199

Huang Z, Wu Y, Zhou X, Xu J, Zhu W, Shu Y, Liu P (2014) Efficacy of therapy with bortezomib in solid tumors: a review based on 32 clinical trials. Future Oncol 10:1795–1807

Hui KF, Chiang AK (2014) Combination of proteasome and class I HDAC inhibitors induces apoptosis of NPC cells through an HDAC6-independent ER stress-induced mechanism. Int J Cancer 135:2950–2961

Karthik S, Sankar R, Varunkumar K, Anusha C, Ravikumar V (2015) Blocking NF-kappaB sensitizes non-small cell lung cancer cells to histone deacetylase inhibitor induced extrinsic apoptosis through generation of reactive oxygen species. Biomed Pharmacother 69:337–344

Kawaguchi Y, Kovacs JJ, McLaurin A, Vance JM, Ito A, Yao TP (2003) The deacetylase HDAC6 regulates aggresome formation and cell viability in response to misfolded protein stress. Cell 115:727–738

Lee AS (2005) The ER chaperone and signaling regulator GRP78/BiP as a monitor of endoplasmic reticulum stress. Methods 35:373–381

Ling YH et al (2002) PS-341, a novel proteasome inhibitor, induces Bcl-2 phosphorylation and cleavage in association with G2-M phase arrest and apoptosis. Mol Cancer Ther 1:841–849

Moriya S et al (2013) Macrolide antibiotics block autophagy flux and sensitize to bortezomib via endoplasmic reticulum stress-mediated CHOP induction in myeloma cells. Int J Oncol 42:1541–1550

Nawrocki ST et al (2006) Aggresome disruption: a novel strategy to enhance bortezomib-induced apoptosis in pancreatic cancer cells. Cancer Res 66:3773–3781

Pandey UB, Batlevi Y, Baehrecke EH, Taylor JP (2007) HDAC6 at the intersection of autophagy, the ubiquitin-proteasome system and neurodegeneration. Autophagy 3:643–645

Su CY, Chong KY, Owen OE, Dillmann WH, Chang C, Lai CC (1998) Constitutive and inducible hsp70 s are involved in oxidative resistance evoked by heat shock or ethanol. J Mol Cell Cardiol 30:587–598

Teicher BA, Ara G, Herbst R, Palombella VJ, Adams J (1999) The proteasome inhibitor PS-341 in cancer therapy. Clin Cancer Res 5:2638–2645

Traynor AM et al (2009) Vorinostat (NSC# 701852) in patients with relapsed non-small cell lung cancer: a Wisconsin oncology network phase II study. J Thorac Oncol 4:522–526

Zang Y, Kirk CJ, Johnson DE (2014) Carfilzomib and oprozomib synergize with histone deacetylase inhibitors in head and neck squamous cell carcinoma models of acquired resistance to proteasome inhibitors. Cancer Biol Ther 15:1142–1152